A cyano-based octanuclear $\{Fe^{III}_4Ni^{II}_4\}$ single-molecule magnet†

Yuanzhu Zhang,[a] Uma Prasad Mallik,[a] Nigam Rath,[a] Gordon T. Yee,[b] Rodolphe Clérac*[cd] and Stephen M. Holmes*[a]

Received 10th March 2010, Accepted 14th May 2010
First published as an Advance Article on the web 4th June 2010
DOI: 10.1039/c0cc00317d

A new low symmetry octanuclear cyano-based $\{Fe^{III}_4Ni^{II}_4\}$ single-molecule magnet (SMM) is described. This SMM exhibits the highest energy barrier ($\Delta/k_B \approx 33$ K) for magnetization reversal seen for any first-row cyanide-based complex. The importance of anisotropy axes alignment and their impact on SMM properties are illustrated when cubic $\{Fe^{III}_4Ni^{II}_4\}$ boxes are compared to octanuclear complexes of lower overall symmetry.

Single-molecule magnets (SMMs) are an unusual class of complexes that have received considerable attention over the last decade due to their superparamagnetic-like properties. The most celebrated class of SMMs are those containing transition metal centers linked *via* oxo- and carboxylate bridges, with $\{Mn_{12}O_{12}(OAc)_{16}(OH_2)_4\}$ being the most famous example.[1] Due to the presence of a large spin ground state (S_T) and uniaxial Ising-like magnetic anisotropy ($D < 0$ considering the following Hamiltonian: $H = DS_{T,z}^2$), these molecular objects exhibit a substantial energy barrier to magnetization reversal ($\Delta = |D|S_T^2$ or $\Delta = |D|(S_T^2 - \frac{1}{4})$ for integer or half-integer S_T values, respectively). With sufficiently large barriers, slow relaxation of the magnetization can be observed at temperatures well above 2 K. Of known SMM complexes, $[Mn^{III}_6O_2(Et\text{-}sao)_6(O_2CPhMe_2)_2(EtOH)_6]$ displays the largest energy barrier (86 K) seen to date.[1h]

Among polynuclear complexes that exhibit slow relaxation of the magnetization those containing cyanide bridges represent a relatively unexplored class of SMMs.[2–5] These cyanometalate SMM systems are usually designed using a premeditated assembly of paramagnetic building-blocks that exhibit substantial orbital angular momentum contributions to their spin ground state. The most common building-blocks are those derived from $[fac\text{-}LM(CN)_3]^{n-}$ ions, where L is a variety of mono- and tridentate ligands.[3–5] Several reports suggest that the magnetic anisotropy and energy barriers to magnetization reversal may be enhanced upon lowering the overall symmetry of polynuclear cyanometalates.[4a,f–h,5d] Using strategies reminiscent of oxo-carboxylate SMMs, we previously reported that the overall magnetic anisotropy of cyanide-bridged tri- and tetranuclear complexes may be enhanced upon parallel alignment of the anisotropy tensors of the $[(Tp^R)Fe^{III}(CN)_3]^-$ anions.[4a,e–g,5d] In comparison, the magnetization reversal barrier is enhanced upon conversion of cubic $\{Fe^{III}_6Cu^{II}_8\}$ complexes ($\Delta/k_B = 11.3$ K) to trigonal bipyramidal $\{Fe^{III}_2Cu^{II}_3\}$ ($\Delta/k_B = 23.2$ K). *Via* symmetry reduction, the formerly octahedral complexes become C_{3v}-symmetric, and the three-fold rotation axes of the $[(Tp^R)Fe^{III}(CN)_3]^-$ building-blocks become approximately collinear, affording an efficient alignment of the anisotropy tensors.[4,5d] In the present report, we focus on a new low symmetry octanuclear $\{Fe^{III}_4Ni^{II}_4\}$ complex that can be considered as an unzipped version of previously reported cubic SMMs.[4b,d] This compound illustrates how molecular symmetry, connectivity, and magnetic properties of an octanuclear complex may be modified by ancillary ligands choice.

Treatment of $[NEt_4][(Tp^{*Me})Fe^{III}(CN)_3]\cdot H_2O$ (**1**, Fig. S1, ESI†) [Tp^{*Me} = tris(3,4,5-trimethylpyrazolyl)borate] with nickel(II) perchlorate and tris(2-aminomethyl)amine (tren) in methanol affords $\{[(Tp^{*Me})Fe^{III}(CN)_3]_4[Ni^{II}(tren)]_4[ClO_4]_4\}\cdot 7H_2O\cdot 4MeCN$ (**2**) as red plates after 7 days.‡ The infrared spectrum of **2** exhibits intense $\tilde{\nu}_{BH}$ (2541 cm^{-1}) and four different $\tilde{\nu}_{CN}$ (2156, 2141, 2130, 2114 cm^{-1}) stretches that are shifted in energies relative to those seen for **1** (2554, $\tilde{\nu}_{BH}$; 2119, 2115 cm^{-1}, $\tilde{\nu}_{CN}$), suggesting bridging and terminal cyanides are present.[4,5a–d]

Compound **2** crystallizes as a tetra-cationic octanuclear species in the triclinic $P\bar{1}$ space group (Fig. 1 and Fig. S2–S4, ESI†).§ The polynuclear complex consists of two

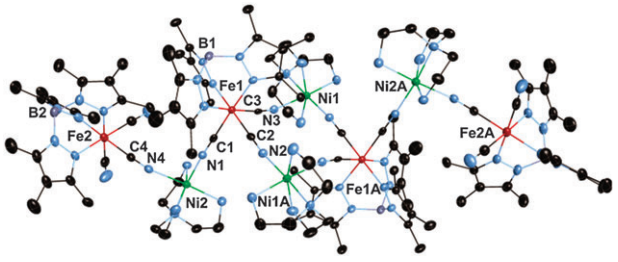

Fig. 1 X-Ray structure of **2**. Thermal ellipsoids are at the 50% level, and all anions, lattice solvent, and hydrogen atoms are eliminated for clarity. Selected bond distances (Å) and angles (°): Fe1–C1 1.921(4), Fe1–C3 1.935(4), Ni1–N2 2.038(4), Ni1–N3A 2.132(4), C1–Fe1–C2 86.2(2), Ni1–N3–C3 158.7(4), Ni1–N2–C2 170.6(3), N2–Ni1–N3 89.9(4).

[a] *Department of Chemistry and Biochemistry, University of Missouri-St. Louis, St. Louis, Missouri 63121, USA. E-mail: holmesst@umsl.edu; Fax: +1 314 516 5342; Tel: +1 314 516 4382*
[b] *Department of Chemistry, Virginia Polytechnic and State University, Blacksburg, Virginia 24061, USA*
[c] *CNRS, UPR 8641, Centre de Recherche Paul Pascal (CRPP), Equipe "Matériaux Moléculaires Magnétiques", 115 avenue du Dr Albert Schweitzer, Pessac, F-33600, France E-mail: clerac@crpp-bordeaux.cnrs.fr; Fax: +33 5 56 84 56 00; Tel: +33 5 56 84 56 50*
[d] *Université de Bordeaux, UPR 8641, Pessac, F-33600, France*
† Electronic supplementary information (ESI) available: Additional synthetic details, structural, and magnetic data for **1** and **2**. CCDC 768189 (**1**) and 768190 (**2**). For ESI and crystallographic data in CIF or other electronic format see DOI: 10.1039/c0cc00317d

crystallographically independent Fe^{III} (Fe1 and Fe2) and Ni^{II} (Ni1 and Ni2) ions that are linked *via* cyanide bridges to form a central $\{Fe^{III}_2Ni^{II}_2\}$ square linked to two adjacent bimetallic $\{Fe^{III}Ni^{II}\}$ units (Fig. 1 and Fig. S2, ESI†). The transition metal centers adopt distorted octahedral geometries and exhibit Fe–C [1.919(4) to 1.935(4) Å] and Ni–N [2.038(4) and 2.132(4) Å] bond lengths that are within the typical ranges. The bridging cyanides range from nearly linear [179.4(4)° for Fe1–C1–N1] to bent [158.7(4)° for Ni1–N3–C3] indicating that the complex has low overall symmetry. Nearly parallel orientation of the pseudo-C_3 rotation axes for the Fe^{III} sites (Fig. 1) suggests that a favorable (*i.e.* for SMM properties) alignment of the anisotropy tensors is likely present in **2**.[4f,5d,6]

To probe this hypothesis a series of magnetic measurements were conducted.¶ The temperature dependence of the χT product for **2** indicates that the Fe^{III} and Ni^{II} centers interact in ferromagnetic manner. Consistent with this assumption, the χT values increase from 8.7 cm^3 K mol^{-1} at 300 K, towards a maximum value of *ca.* 25.5 cm^3 K mol^{-1} at 5 K; below 5 K, χT decreases to 21.1 cm^3 K mol^{-1} at 1.8 K (Fig. 2 and Fig. S6, ESI†). From the structure of **2**, the magnetic data were simulated with MAGPACK[7] using an isotropic Heisenberg Hamiltonian $H = -2J[S_{Ni2}(S_{Fe2} + S_{Fe1}) + (S_{Fe1} + S_{Fe1A})\text{-}(S_{Ni1} + S_{Ni1A}) + S_{Ni2A}(S_{Fe2A} + S_{Fe1A})]$, where J represents the average exchange between Fe^{III}_{LS} ($S = \frac{1}{2}$) and Ni^{II} ($S = 1$) spins over the four different Fe–CN–Ni magnetic pathways present (by symmetry) within the $\{Fe^{III}_4Ni^{II}_4\}$ core, and S_i is the spin operator of each metal ion. An adequate simulation of the data was obtained between 300 and 15 K and J/k_B and $g_{avg.}$ are found to be +9.5(1) K and 2.4(1), respectively, suggesting an $S_T = 6$ spin ground state for **2**; these values compare favorably to a variety of other tri-, tetra-, and octanuclear $\{Fe^{III}_nNi^{II}_m\}$ complexes containing anisotropic $[(Tp^R)Fe^{III}(CN)_3]^-$ anions ($2.7 \leq g_{Fe} \leq 3.1$; see ESI†).[4,5a–d] We note that within our model, consideration of two different (or more) magnetic interactions, different g factors for Fe^{III} and Ni^{II}, or local magnetic anisotropy on the Fe^{III} and Ni^{II} metal ions does not improve the quality of the simulation or enable magnetic data incorporation below *ca.* 15 K. We infer that a combination of some or all of the above factors are likely responsible for the magnetic behavior seen below *ca.* 15 K.

The field dependences of the magnetization below 6 K (Fig. 2 inset and Fig. S7, ESI†) indicate that **2** adopts an $S_T = 6$ spin ground state. The magnetization of **2** does not saturate (at 7 T and 1.8 K) and reaches a maximum value of 12.6 μ_B that is consistent with an $S_T = 6$ spin ground state (with $g > 2$) consisting of a 4 : 4 ratio of ferromagnetically coupled Ni^{II} and Fe^{III}_{LS} ions. Further assuming that uniaxial magnetic anisotropy is present in **2**, the M *vs.* H/T data below 6 K were fitted well using an $H = DS_{T,z}^2$ Hamiltonian (inset, Fig. 2) and considering an $S_T = 6$ ground state. The D/k_B and g values are estimated to be −1.29(2) K and 2.60(5), respectively, and differ markedly from those seen for $S_T = 6$ cubic $\{Fe^{III}_4Ni^{II}_4\}$ complexes [−0.33 K and 2.2].[4b,d] This macro-spin model confirms unambiguously the $S_T = 6$ spin ground state for **2** and also its large observed uniaxial anisotropy. It is also worth mentioning that no hysteresis was observed in the M *vs.* H data above 1.8 K (Fig. S7, ESI†).

Remarkably, the ac susceptibility above 1.8 K is frequency-dependent in both in-phase (χ') and out-of-phase (χ'') components (Fig. 3 and Fig. S8–S10, ESI†) for **2**. The relaxation time, deduced from the temperature and frequency dependence of the ac susceptibility, follows thermally activated behavior (inset, Fig. 3). The barrier to magnetization reversal is estimated to be about 33 K and is significantly lower than the theoretical value anticipated from $|D|S_T^2 = 46$ K. Under the assumption that quantum tunneling of the magnetization (QTM) might be responsible for this difference, the ac susceptibility was measured under small dc fields to lift the energy level degeneracy and thus minimize the QTM pathways for relaxation. As expected the application of a dc magnetic field (up to 800 Oe, Fig. S11, ESI†) reduces the characteristic frequency at 1.9 K from 2.4 to 1.3 Hz, confirming that QTM is operative.[4b,d,g,h]

In summary, we have described that the magnetic anisotropy and relaxation dynamics are critically sensitive to the overall structure in $\{Fe^{III}_4Ni^{II}_4\}$ complexes. As far as we know, the energy barrier for magnetization reversal in **2** is the highest seen for any first-row cyanometalate SMM and is the second largest for *any* cyanide-based complex.[2c,5d,5e] Future efforts

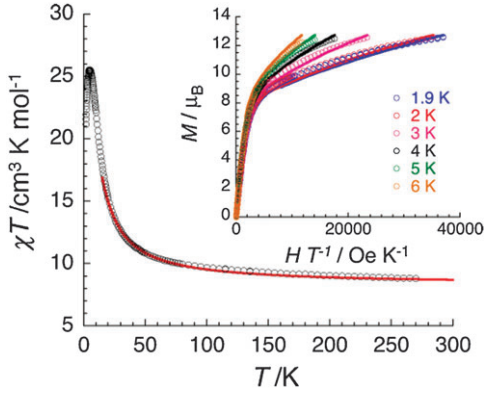

Fig. 2 χT *vs.* T data for **2** at $H_{dc} = 0.1$ T (with χ defined as the molar magnetic susceptibility equal to M/H). Inset: magnetization *vs.* H/T between 1.9 and 6 K. Solid lines represent least-squares fitting of the data to an anisotropic $S_T = 6$ macro-spin model (see text).

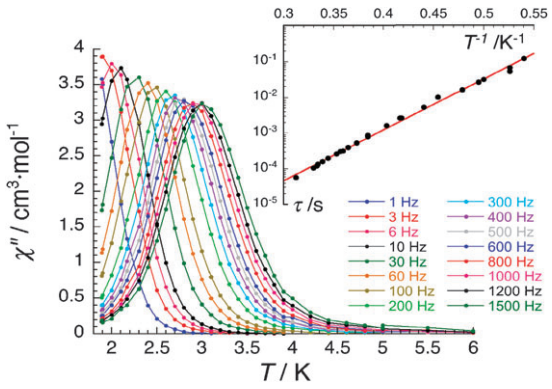

Fig. 3 χ'' *vs.* T data for **2** below 6 K at various ac frequencies ($H_{dc} = 0$ Oe; $H_{ac} = 3$ Oe). Inset: semi-logarithmic τ *vs.* T^{-1} plot for **2**. Red solid line is best simulation of data using an Arrhenius law (with $\tau_0 = 2.5 \times 10^{-9}$ s).

will explore incorporation of 4d and 5d ions into this and other cyano-based systems.

S.M.H. gratefully acknowledges the National Science Foundation (CHE 0914935, CAREER; CHE 0939987, X-ray upgrade) and University of Missouri-St. Louis for financial support. G.T.Y. thanks the National Science Foundation (CHE 0210395); and R.C. acknowledges the University of Bordeaux, the ANR (NT09_469563, AC-MAGnets project), the Région Aquitaine, the GIS Advanced Materials in Aquitaine (COMET Project), MAGMANet (NMP3-CT-2005-515767), and the CNRS (PICS N°4659) for financial support.

Notes and references

‡ Synthesis of **1**: drop wise addition of aqueous 30% H_2O_2 (20 mL) into a 4 : 1 CH_2Cl_2/^{i}PrOH (v/v, 50 mL) solution of $[NEt_4]_2[(Tp^{*Me})Fe^{II}(CN)_3]\cdot H_2O$ (3.05 g, 4.06 mmol, see ESI†) over 30 min afforded a red mixture. After 3 h, the aqueous phase was decanted and the organic phase dried over anhydrous $MgSO_4$. The red-brown mixture was filtered and the filtrate concentrated under vacuum to *ca.* 10 mL. Addition of Et_2O (60 mL) afforded a red powder. Yield: 1.75 g (69.3%). Red tablets are obtained *via* slow evaporation of 2 : 1 MeOH/H_2O solutions of **1**. Anal. calcd for $C_{29}H_{50}BFeN_{10}O$: C, 56.05; H, 8.11; N, 22.54%. Found: C, 56.05; H, 7.90; N, 22.46%. IR (Nujol, cm^{-1}): 2544 ($\tilde{\nu}_{BH}$, m), 2119 ($\tilde{\nu}_{CN}$, m), 2115 ($\tilde{\nu}_{CN}$, m). Synthesis of **2**: under an argon atmosphere, treatment of $[Ni(OH_2)_6][ClO_4]_2$ (73.0 mg, 0.200 mmol) with tren (30.5 mg, 0.209 mmol) in 1 : 1 (v/v) MeCN/MeOH (10 mL) afforded a purple mixture that was stirred for 10 min. A solution of **1** (124.5 mg, 0.200 mmol) in methanol (10 mL) was added and the resulting dark red mixture was filtered and allowed to stand for one week. Dark red tablets were isolated *via* suction filtration, washed with Et_2O (2 × 5 mL), and dried under vacuum for 2 min at room temperature. Yield: 84.0 mg (49.4%). Anal. calcd for $\{[(Tp^{*Me})Fe^{III}(CN)_3]_4[Ni^{II}(tren)]_4[ClO_4]_4\}\cdot 7H_2O\cdot MeCN$: $C_{112}Cl_4H_{204}N_{54}O_{23}B_4Fe_4Ni_4$: C, 40.31; H, 6.18; N, 22.65%. Found: C, 40.30; H, 6.35; N, 22.56%. IR (Nujol, cm^{-1}): 3383 (m), 3351 (m), 3304 (m), 2740 (w), 2541 (m), 2251 (w), 2156 (s), 2141 (m), 2130 (s), 2114 (m), 1604 (m), 1562 (w), 1516 (m), 1365 (s), 1243 (vs), 1173 (m), 1098 (vs), 1049 (s), 1027 (s), 998 (s), 979 (s), 930 (w), 883 (m), 874 (m), 834 (m), 736 (m), 690 (w), 667 (w), 651 (w), 625 (s), 606 (w), 561 (w), 540 (m).

§ Crystallographic data for **1** and **2** were collected on a Bruker Apex II diffractometer using graphite-monochromated MoKα radiation. All structures were solved by direct methods and refined against all data using SHELX-97.[8] Crystal data for **1**: $C_{29}H_{50}BFeN_{10}O$, M = 621.45, monoclinic space group, $P2_1/n$, Z = 4, a = 9.9051(6) Å, b = 16.122(1) Å, c = 20.399(1) Å, α = 90°, β = 93.661(2)°, γ = 90°, V = 3250.8(4) Å^3, D_c = 1.270 g cm^{-3}, μ = 0.503 mm^{-1}, R_1 = 0.0447, wR_2 = 0.1414. Crystal data for **2**: $C_{58}H_{105}B_2Cl_2Fe_2N_{28}Ni_2O_{11.5}$, M = 1700.34, $P\bar{1}$, Z = 1, a = 14.058(1) Å, b = 14.568(1) Å, c = 23.412(2) Å, α = 75.052(3)°, β = 77.373(3)°, γ = 62.117(3)°, V = 4067.5(5) Å^3, D_c = 1.338 g cm^{-3}, μ = 0.941 mm^{-1}, R_1 = 0.0622, wR_2 = 0.1598. CCDC 768189 (**1**) and 768190 (**2**).

¶ Magnetic measurements were conducted on a Quantum Design MPMS-XL SQUID magnetometer equipped with a 7 T magnet. The magnetic data were corrected for the sample holder and the diamagnetic contributions. For additional magnetic data see ESI.†

1 (*a*) M. N. Leuenberger and D. Loss, *Nature*, 2001, **410**, 789–793; (*b*) A. Caneschi, A. D. Gatteschi, R. Sessoli, A. L. Barra, L. C. Brunel and M. Guillot, *J. Am. Chem. Soc.*, 1991, **113**, 5873–5874; (*c*) R. Sessoli, H.-L. Tsai, A. R. Schake, S. Wang, J. B. Vincent, K. Folting, D. Gatteschi, G. Christou and D. N. Hendrickson, *J. Am. Chem. Soc.*, 1993, **115**, 1804–1816; (*d*) R. Sessoli, D. Gatteschi, A. Caneschi and M. A. Novak, *Nature*, 1993, **365**, 141–143; (*e*) W. Wernsdorfer, N. Aliaga-Alcalde and G. Christou, *Science*, 2003, **302**, 1015–1018; (*f*) D. Gatteschi and R. Sessoli, *Angew. Chem., Int. Ed.*, 2003, **42**, 268–297 and references therein; (*g*) D. Gatteschi, R. Sessoli and J. Villain, *Molecular nanomagnets*, Oxford University Press, New York, 2006 and references therein; (*h*) C. J. Milios, A. Vinslava, W. Wernsdorfer, S. Moggach, S. Parsons, S. P. Perlepes, G. Christou and E. K. Brechin, *J. Am. Chem. Soc.*, 2007, **129**, 2754–2755.

2 (*a*) J. J. Sokol, A. G. Hee and J. R. Long, *J. Am. Chem. Soc.*, 2002, **124**, 7656–7657; (*b*) L. M. C. Beltran and J. R. Long, *Acc. Chem. Res.*, 2005, **38**, 325–334; (*c*) D. E. Freedman, D. M. Jenkins, A. T. Iavarone and J. R. Long, *J. Am. Chem. Soc.*, 2008, **130**, 2884–2885; (*d*) M. Ferbinteanu, H. Miyasaka, W. Wernsdorfer, K. Nakata, K. Sugiura, M. Yamashita, C. Coulon and R. Clérac, *J. Am. Chem. Soc.*, 2005, **127**, 3090–3099.

3 (*a*) C. P. Berlinguette, D. Vaughn, C. Canada-Vilalta, J. R. Gálan-Mascarós and K. R. Dunbar, *Angew. Chem., Int. Ed.*, 2003, **42**, 1523–1526; (*b*) E. J. Schelter, F. Karadas, C. Avendano, A. Prosvirin, W. Wernsdorfer and K. R. Dunbar, *J. Am. Chem. Soc.*, 2007, **129**, 8139–8149; (*c*) M. Shatruk, A. Dragulescu-Andrasi, K. E. Chambers, S. A. Stoian, E. L. Bominaar, C. Achim and K. R. Dunbar, *J. Am. Chem. Soc.*, 2007, **129**, 6104–6116.

4 (*a*) D. Li, G. Wang, G. T. Yee, A. V. Prosvirin and S. M. Holmes, *Inorg. Chem.*, 2005, **44**, 4903–4905; (*b*) D. Li, S. Parkin, G. Wang, G. T. Yee, R. Clérac, W. Wernsdorfer and S. M. Holmes, *J. Am. Chem. Soc.*, 2006, **128**, 4214–4215; (*c*) D. Li, S. Parkin, G. Wang, G. T. Yee and S. M. Holmes, *Inorg. Chem.*, 2006, **45**, 1951–1959; (*d*) D. Li, R. Clérac, S. Parkin, G. Wang, G. T. Yee and S. M. Holmes, *Inorg. Chem.*, 2006, **45**, 7569–7571; (*e*) D. Li, S. Parkin, G. Wang, G. T. Yee and S. M. Holmes, *Inorg. Chem.*, 2006, **45**, 2773–2775; (*f*) K. Park and S. M. Holmes, *Phys. Rev. B: Condens. Matter Mater. Phys.*, 2006, **74**, 224440; (*g*) D. Li, R. Clérac, G. Wang, G. T. Yee and S. M. Holmes, *Inorg. Chem.*, 2006, **45**, 5251–5253; (*h*) D. Li, R. Clérac, G. Wang, G. T. Yee and S. M. Holmes, *Eur. J. Inorg. Chem.*, 2007, 1341–1346.

5 (*a*) S. Wang, J.-L. Zuo, H.-C. Zhou, H. J. Choi, Y. X. Ke, J. R. Long and X.-Z. You, *Angew. Chem., Int. Ed.*, 2004, **43**, 5940–5943; (*b*) J. Kim, S. Han, I.-K. Cho, K. Y. Choi, M. Heu, S. Yoon and B. J. Suh, *Polyhedron*, 2004, **23**, 1333–1339; (*c*) S. Wang, J.-L. Zuo, H.-C. Zhou, Y. Song, S. Gao and X.-Z. You, *Eur. J. Inorg. Chem.*, 2004, 3681–3687; (*d*) C.-F. Wang, J.-L. Zuo, B. M. Bartlett, Y. Song, J. R. Long and X.-Z. You, *J. Am. Chem. Soc.*, 2006, **128**, 7162–7163; (*e*) J. H. Yoon, J. H. Lim, H. C. Kim and C. S. Hong, *Inorg. Chem.*, 2006, **45**, 9613–9615.

6 (*a*) D. Gatteschi and L. Sorace, *J. Solid State Chem.*, 2001, **159**, 253–261; (*b*) H. Oshio and M. Nakano, *Chem.–Eur. J.*, 2005, **11**, 5178–5185.

7 (*a*) J. J. Borrás-Almenar, J. M. Clemente-Juan, E. Coronado and B. S. Tsukerblat, *Inorg. Chem.*, 1999, **38**, 6081–6088; (*b*) J. J. Borrás-Almenar, J. M. Clemente-Juan, E. Coronado and B. S. Tsukerblat, *J. Comput. Chem.*, 2001, **22**, 985–991.

8 G. M. Sheldrick, *SHELX-97, Program for refinement of crystal structures*, University of Göttingen, Germany, 1997.